

Published in final edited form as:

Microvasc Res. 2011 November ; 82(3): 210–220. doi:10.1016/j.mvr.2011.06.013.

Microfluidic devices for modeling cell-cell and particle-cell interactions in the microvasculature

Balabhaskar Prabhakarandian^{1,2}, Ming-Che Shen¹, Kapil Pant¹, and Mohammad F. Kiani^{2,3}

¹Biomedical Technology, CFD Research Corporation, 215 Wynn Dr. Huntsville AL 35805

²Department of Mechanical Engineering, Temple University, Philadelphia PA 19122

³Department of Radiation Oncology, Temple University, Philadelphia PA 19122

Abstract

Cell-fluid and cell-cell interactions are critical components of many physiological and pathological conditions in the microvasculature. Similarly, particle-cell interactions play an important role in targeted delivery of therapeutics to tissue. Development of in vitro fluidic devices to mimic these microcirculatory processes has been a critical step forward in our understanding of the inflammatory process, development of nano-particulate drug carriers, and developing realistic in vitro models of the microvasculature and its surrounding tissue. However, widely used parallel plate flow based devices and assays have a number of important limitations for studying the physiological conditions in vivo. In addition, these devices are resource hungry and time consuming for performing various assays. Recently developed, more realistic, microfluidic based devices have been able to overcome many of these limitations. In this review, an overview of the fluidic devices and their use in studying the effects of shear forces on cell-cell and cell-particle interactions is presented. In addition, use of mathematical models and Computational Fluid Dynamics (CFD) based models for interpreting the complex flow patterns in the microvasculature are highlighted. Finally, the potential of 3D microfluidic devices and imaging for better representing in vivo conditions under which cell-cell and cell-particle interactions take place are discussed.

1. Introduction

Microvascular networks are generally defined as a series of interconnected arterioles (10–100 μm), capillaries (2–10 μm), and venules (20–100 μm) which work as a functional unit and are often the key sites for many of the cell-cell and particle-cell interactions during physiological and/or pathological processes (Granger et al., 2010; Totani and Evangelista, 2010). These cell-cell interactions include the leukocyte adhesion cascade (Ley et al., 2007), which includes leukocyte rolling, adhesion to the endothelium and subsequent migration into the tissue, platelet adhesion (Jackson et al., 2009), and tumor cell adhesion (Zigler et al., 2010). Recent advances in targeted drug delivery to the microvasculature often involves encapsulating drugs in delivery vehicles ranging from microparticles (Kendall et al., 2009),

© 2010 Elsevier Inc. All rights reserved.

Corresponding author: Mohammad F. Kiani, Ph.D., F.A.H.A., Professor and Chair, Department of Mechanical Engineering, Temple University, 1947 N. 12th St., Philadelphia, PA 19122, Phone: (215) 204-4644, Fax: (215) 204-4956, mkiani@temple.edu.

Publisher's Disclaimer: This is a PDF file of an unedited manuscript that has been accepted for publication. As a service to our customers we are providing this early version of the manuscript. The manuscript will undergo copyediting, typesetting, and review of the resulting proof before it is published in its final citable form. Please note that during the production process errors may be discovered which could affect the content, and all legal disclaimers that apply to the journal pertain.

to nanoparticles (Petrelli et al., 2010), liposomes (Zhai et al., 2010; Scott et al., 2009; Patillo et al., 2009) and virus (Mateu 2011) based delivery systems. With the advent of biodegradable particles (Kumari et al., 2010), and novel methodologies such as particle shape modification (Doshi et al., 2010; Champion et al., 2009) and the use of empty red blood cells (Muzykantov 2010) for drug delivery, a robust *in vitro* platform for assessing drug delivery is desired. Successful delivery of these particles to the target tissue, as well as interaction of blood cells with the endothelium, depends significantly upon their interaction with and subsequent firm adhesion to the vascular endothelium. This process is primarily dependent on three major components: (a) the biological make-up of the ligands on cells/particles and their corresponding receptors on the endothelium, (b) associated local hemodynamic factors such as wall shear rate and residence time which are often dependent on the geometric features of the local microvasculature, and (c) the differential biodistribution of cells/particles between normal and the diseased tissue.

Significant progress has been made since the early 1990's in our understanding of the biological receptors and their corresponding ligands using a combination of cell staining techniques. Pioneering work in the field of cell adhesion as summarized in Bevilacqua, 1993 and Carlos et al., 1994 resulted in the discovery of adhesion molecules such as E-Selectin and ICAM-1 which are key players influencing leukocyte adhesion to the endothelium. Traditionally *in vitro* studies of cell-cell and particle-cell interactions in the microcirculation involves static assays in which particles are incubated on protein matrices or adherent cells in tissue culture dishes. Following a specified incubation time and number of washes, the number of adherent particles is quantified. This procedure is still commonly used for characterizing particle adhesion (Butler et al., 2009; Humphries 2009; Paprocka et al., 2008; Peramo et al., 2008) and has provided significant insight into the biochemical processes responsible for mediating the adhesion phenomena. However, a key component lacking in these static assays is the physiological fluid flow and its relationship to particle adhesion.

To address the lack of physiological fluid flow during particle adhesion studies, *in-vitro* flow chambers were developed. A common feature of these flow chambers is a transparent apparatus and perfusion of a suspension of particles at low Reynolds numbers to match wall shear rates observed in blood vessels *in-vivo*. The vessel wall is modeled by either coating biomolecules or growing cells on the lower plate of the flow chamber (Luscinskas et al., 1994). Particles are then perfused at desired range of flow rates to quantify the number of adhering particles under various shear rates. These devices have been predominantly used to study leukocyte-endothelial cell interactions (Prabhakarbandian et al., 2001; Crutchfield et al., 2000; Patel 1999; Goetz et al., 1994; Cozens-Roberts et al., 1990; Lawrence et al., 1987) and tumor-endothelial cell interactions (Alves et al., 2008, Burdick et al., 2001, Aigner et al., 1998; Tözeren et al., 1995). In the early 2000's, several research groups began using parallel plate flow chambers to develop targeted drug delivery systems consisting of micro/nanoparticle formulations coated with ligands to corresponding receptors on the endothelial cells (Sakhalkar et al., 2003; Blackwell et al., 2001; Dickerson et al., 2001; Kiani et al., 2002). However, use of parallel plate flow chambers to study and validate these drug carriers is rather expensive and time consuming. Parallel plate flow chambers often require large volumes of reagents due to their large size and can usually model one set of flow rates per experiment. In addition, these systems often do not accurately model geometrical features (e.g., bifurcations, stenoses) and flow conditions (e.g., converging or diverging flows at bifurcations) that are present *in vivo*.

Creation of fluidic devices which accurately reproduce *in vivo* features and analysis of the complex flow patterns in these devices require synergistic development of two exciting technologies of the 21st century. First, microfabrication techniques (Anderson et al., 2000) such as soft-lithography, laser etching, and hot embossing have resulted in the development

of microfluidic devices that can better reproduce micrometer features of microvasculature (van der Meer et al., 2010; Barber & Emerson 2010). Second, development of Computational Fluid Dynamic (CFD)-based modeling provides an ideal methodology for understanding and analyzing the complex flow patterns in these devices. The main goal of this review is to present an overview of the fluidic devices for analyzing cell-cell and particle-cell interactions and the methodologies that are used to analyze findings from these devices.

2. Cell-Cell and Particle-Cell Adhesion

Cell-cell and particle-cell interaction is a key step for ensuring proper cell-cell communication and targeted delivery of drug particles (Kang et al., 2011). Of all the cell-cell interactions, leukocyte adhesion to the vascular endothelium is the most fundamental and best understood process. The movement of leukocytes from within the vasculature to the extravascular space involves a well orchestrated set of adhesion events (Kansas 1996; Springer 1994; Luscinskas and Gimbrone, 1996) and is mediated, in part, by adhesive bonds which form between glycoproteins (ligands) present on the leukocytes and cognate glycoproteins (receptors) present on the endothelium. A key paradigm in this adhesion cascade is that certain endothelial cell adhesion molecules are inducible. That is, they are expressed at a low level, if at all, on endothelium within normal tissue, but are dramatically upregulated in response to appropriate biochemical stimuli (e.g. cytokines such as IL-1 β). Thus, in response to various stimuli, the endothelium becomes activated and increases its expression of receptors (adhesion molecules) that bind ligands on the leukocytes. Leukocytes attach to the endothelium, for the most part via the selectins, and begin to translate along the vessel wall (roll) at a velocity which is significantly lower than leukocytes in the free stream (Springer 1994). As the leukocytes roll they become activated in response to chemokines (Springer 1994; Ebnet and Vestweber, 1999). The activation involves a number of changes to the leukocytes including an alteration in the density of the integrins (Diamond and Springer, 1994; Newton et al., 1994) on the leukocyte surface as well as an increase in the “stickiness” (a conformational change) of the integrins for their cognate endothelial cell adhesion molecules (e.g. ICAM-1). Figure 1a shows a schematic of this cascade and Figure 1b shows the biophysical forces that guide this interaction. When the adhesive bond strength is smaller than the shear forces, leukocytes tend to roll. However, once the bond forces overtake the shear forces, the leukocytes adhere firmly via the integrins and proceed to migrate between adjacent endothelial cells into the extravascular space. A similar process also accounts for platelet adhesion where the interaction of circulating platelets with the vessel wall involves a process of rolling and firm adhesion, leading to thrombus formation.

Several investigators have developed mathematical models to understand the complex cell adhesion cascade. These include the pioneering work of Hammer & Lauffenburger, 1989, 1987 who developed an analytical expression for the shear rate and adhesive force relationship in flow chambers. Their work was further developed into a probabilistic model by Cozens-Roberts et al., 1990 which calculated the probability of the number of bonds between a cell ligand and the surface receptor at a given time resulting in the concept of critical shear rate dependent adhesion model. In addition, this probability based model allowed for transient and continuous study of the attachment and detachment phenomenon. Hammer and Apte, 1992 extended the probability based model by inclusion of the adhesion modulating parameter known as “the fractional spring slippage”, which relates the strain of a bond directly to the rate of bond rupture. They also validated this model by comparing the analysis with the experimental neutrophil adhesive behavior on selectin-coated surfaces in a parallel plate flow chamber.

Although several models have been developed to study the biochemical process of receptor-ligand interaction (Goetz et al., 1994; Simon and Goldsmith 2002) and the hemodynamic impact on adhesion (Chapman and Cokelet, 1996, 1997), the seminal work of Chang et al., 2000, which developed the concept of the “Adhesive Dynamics” methodology, resulted in a global map of the biophysical properties of the adhesion molecules involved in cell-cell interactions. This model also accounted for on/off rates for the receptor-ligand bonds, bond elasticity and the bond lengths. This model was subsequently modified by Bhatia et al., 2003 to incorporate two receptor-ligand interactions comprising of the selectin and integrin components. It was further validated by comparing the predicted rolling velocities of leukocytes with experimental data obtained from parallel plate flow chambers.

3. Flow Chambers

Since the introduction of parallel plate flow chambers by Lawrence et al., 1987 there has been a plethora of changes (Jones et al., 1996) to these systems in attempts to make them more representative of the in vivo conditions and easier to use. However, there is currently only one commercially available parallel plate flow chamber system by Glycotech (Gaithersburg, Maryland, USA). This device normally utilizes a 35mm petri dish for cell culture or receptor coating. Following coating of desired substrate or cell culture, a gasket with a flow path is assembled on top of the dish followed by the device. The entire set-up is held under vacuum during the course of the experiment. Different shear rates in the flow path of the flow chamber are generated by withdrawing the fluid (containing cells or particles) using a syringe pump (Figure 2). The shear rate (γ) in these flow chambers is a function of volumetric flow rate (Q) set by the syringe pump, and channel dimensions (height (h) and width (w)) of the flow chamber and is given by $\gamma = 6Q/h^2w$

Usually, the number of particles adhered at various shear rates is measured and a shear vs. adhesion plot is generated to determine the effects of shear rate on cell adhesion. These devices however are reagent hungry due to their meso-scale dimensions with the smallest variant having a 0.25cm width and 0.013 cm height. In addition, multiple experimental runs at different shear rates are required for generating the shear vs. adhesion plots. There have been several attempts to develop alternate devices predominantly driven by the need for characterizing the effects of multiple shear rates on cell adhesion during the same experiment. These include a variable height flow chamber (Xiao and Truskey, 1996), a variable width flow chamber (Usami et al., 1993) and a flow chamber with radial steps to create recirculation zones (Chiu et al., 1998) and investigation of multiple shear rates (Cozen-Roberts et al., 1990). In addition, a flow chamber with pulsatile flow (Ruel et al., 1995) and devices with side view (Cao et al., 1998 and Leyton-Mange et al., 2006) for monitoring adhesion were developed. A modification of the Glycotech flow chamber with a recirculation loop to minimize reagent usage was developed by Brown and Larson, 2001. However, none of these improved flow chambers have been commercialized due to the (a) cumbersome fabrication procedures, (b) need for extensive cleaning before experiments, and (c) reagent-hungry experiments.

4. Microfluidic Devices

A number of investigators have taken advantage of advances in the field of MEMS-based microfluidic systems to develop micro-scale flow chambers that more accurately reproduce the in vivo conditions and require significantly lower resources compared to parallel plate flow chambers. An added benefit of these microfluidic devices is the ability to easily control the dimensions including the height and width of the fluidic channels which typically range from few micrometers to 100s of micrometers, thereby reducing reagents used by up to three orders of magnitude (ml to ul). Although, microfluidic devices can be fabricated from a

wide array of materials such as metal, glass, polymers, poly-dimethylsiloxane (PDMS) is the most widely used material for fabrication of microfluidic devices. This material is especially useful for fabricating microfluidic devices for biological studies (Sia and Whitesides 2003) because of its gas permeability, optical transparency, biocompatibility and the ability to be coated with a wide variety of proteins. A process known as soft-lithography is commonly used to fabricate many of these microfluidic devices (Figure 3).

One of the first studies to use microfluidics based flow chamber for cell adhesion assays (Brevig et al., 2003) investigated the interaction of leukocytes under shear flow conditions on cultured endothelial cells. Using a microfluidic chip fabricated from polymethyl methacrylate with dimensions of 5000 (length) \times 5000 (width) \times 40 (height) μm , this group showed that compared to static assays, firm adhesion of leukocytes on endothelial cells was found to be dependent on cytokine-mediated activation. This was due to the fact that basal levels of CD18 allowed adhesion of leukocytes on non-activated endothelial cells whereas adhesion under flow required cytokine activated expression of CD54, CD62E, CD18, MCP-1 and MIP-1 α . Continuing along the adhesion based phenomena, Murthy et al., 2004 developed a microfluidic device for separation of a sub-population of neutrophils using antibody based adhesion under fluidic conditions. This device was fabricated at the microscale level using the variable width concept developed by Usami et al., 1993 with a constant height of 57 μm , inlet width of 5mm and the chamber length of 50mm. Nalayanda et al., 2007 showed that cell adhesion and rolling under physiological flow conditions can be readily controlled by patterning surfaces of microfluidic flow chambers (linear channels ranging from 50–100 μm) with adhesion molecules. Agrawal et al., 2008 used a microfluidic device with six parallel channels for demonstrating chemotaxis on leukocytes from a drop of whole blood (<10 μL) under the influence of different chemokines. Use of microfluidic devices for studying leukocyte interactions with red blood cells was demonstrated by Jain and Munn, 2009 showing that leukocytes preferentially marginate downstream of sudden expansions with red blood cell aggregation enhancing the process. Finally, in a recent study, Kotz et al., 2010 used microfluidic based devices for a clinical assay in which neutrophils isolated directly from whole blood were processed on chip for mRNA and protein extractions for genomic and proteomic studies.

Similar to leukocyte interaction assays, microfluidic devices have also been used for platelet adhesion studies. Tran et al., 2005, studied agonist-induced calcium response in single human platelets using a microfluidic device for identification of signaling pathways. Shen et al., 2008 identified the range of shear rates that limit initiation of coagulation pathways using a combination of surface areas treated with tissue factor protein and native platelets. Neeves et al., 2008 used a microfluidic device comprising of thirteen parallel channels (80 μm (height) \times 100 μm (width)) on a collagen coated surface for studying the effects of signaling molecules on the platelet adhesion. Karunarathne et al., 2009 studied platelet interactions with endothelial cells using an array of linear microfluidic channels (100 μm (depth), 200 μm (width)) which resulted in identification of the dual nature of extracellular ATP as agonist and antagonist of P2X1 receptor (an ATP-gated cation channel). A novel methodology based on localized strain rate micro-gradients in microfluidic devices for measuring platelet function and aggregation was demonstrated by Tovar-Lopez et al., 2010. Results from this assay especially highlight the usefulness of microfluidic devices for understanding the hemodynamic and platelet mechano-transduction mechanisms during platelet aggregation.

Although microfluidic based devices have been used widely for cell based assays, there have been only a limited number of studies using synthetic particles in microfluidic flow chambers. For example, the first such study to our knowledge was by Farokhzad et al., 2005 where they showed that specificity of targeted aptamers can be investigated by using

particles conjugated to aptamers that recognize the transmembrane prostate specific membrane antigen (PSMA). This concept of testing drug particle adhesion was modified by Fillafer et al., 2009 using an acoustically-driven microfluidic device for adhesion of targeted vs. non targeted protein coated microparticles to epithelial cells. While static incubation assays showed little difference in adhesion, fluidic results showed that the non-targeted particles did not bind. These results re-emphasize the need for studying adhesion processes under physiological flow conditions.

Taking advantage of this development in the field of microfluidic devices, several companies are now developing adhesion assays based on microfluidic devices. Notable among these are devices from Ibidi (Germany) and Cellix (Ireland) which allow for the culture of cells and studies of their interactions with cells and/or particles in a microfluidic setting (Figure 4). However, neither of these devices have a high throughput (>24 assays) version that can accelerate the testing and screening process. In this context, a high-throughput device has been developed by Fluxion Biosciences (Conant et al., 2009) for cell assays (Figure 4) by integrating microfluidic constructs with well plates. In spite of all the advancements for performing a wide range of assays, as mentioned before, all of these devices still use idealized channels to model microvessels and do not reproduce the vascular networks as observed in vivo. Nevertheless, they are easy to fabricate and allow the use of simple mathematical formulas for prediction of flow parameters.

5. In Vivo Mimetic Microfluidic Devices

Although though microfluidic devices reduce the reagent consumption significantly, they still fall short of matching even the simplest in vivo features such as bifurcations which are the often the focal points of adhesion of platelets and leukocytes under normal and pathological conditions (Prabhakarpanidjan et al., 2011; Tousi et al., 2010). Furthermore, reproductions of complex geometries of the microvasculature, e.g. diameter variability along the vessel length or stenoses, are often needed to study various microcirculatory flow conditions. Microfluidic devices mimicking simple in vivo characteristics were developed to improve upon the first generation of linear channel microfluidic devices. In vivo mimetic devices can be fabricated as either having idealized geometries (e.g. semi-circular or circular channels in linear chambers) or having more realistic and complex geometries observed in vivo. Before the advent of PDMS based microfluidic devices, Coklet et al., 1993 fabricated the first set of microfluidic devices containing bifurcations using photolithography on glass slides. Their methods of creating approximating circular channels, as well as repeating constructs of diverging bifurcations, allowed for blood flow studies in these complex systems. In a second study, Frame et al., 1995 created semi-circular channels on glass in the range of 20–50 μm and were able to successfully culture endothelial cells in these channels.

During the last few years, microfluidic devices incorporating bifurcations and other physiologically realistic geometries (e.g. stenosis) have been developed using PDMS. These devices have been used to study leukocyte adhesion (Rouleau et al., 2010; Schaff et al., 2007) and platelet adhesion (Tovar-Lopez et al., 2009; Runyon et al., 2004). Simple bifurcating microfluidic devices are now being marketed for cell adhesion assays by commercial entities Cellix Ltd. and Ibidi LLC. To address the need for the development of new methods that can rapidly create channels that mimic the in vivo features of microvascular networks, Borenstein et al., 2010 utilized two semi-circular idealized bifurcating patterns on polystyrene to create circular channels. They also demonstrated successful culture of endothelial cells in the fabricated device. Two other studies (Abdelgawad et al., 2010; Fiddes et al., 2010) developed alternative methodologies for creating circular channels. Both of these studies utilized the concept of polymerization of the liquid silicone oligomers with gas streams to convert rectangular cross-sections into circular

sections (Figure 5). Unlike the study by Borenstein et al., 2010, where the smallest channel diameter was 400 μ m, channels as small as 5 μ m were fabricated using the polymerization methods (Abdelgawad et al., 2010; Fiddes et al., 2010). In addition, endothelial cells were successfully cultured in these devices highlighting the circular patterns of cells.

Research for deciphering the optimal shapes of drug particles (Yoo et al., 2010; Champion et al., 2007) is gaining momentum due to recent findings indicating that shape of the drug particle is critical for drug particle uptake (Muro et al., 2008). Recently, Doshi et al., 2010 showed that a simple bifurcating microfluidic flow chambers can be used to differentiate between the adhesive characteristics of differently shaped drug carrying particles. This study showed that while static assays and linear channels of a microfluidic flow chamber could not resolve the difference between the adhesion patterns of various shaped particles, the bifurcating section (Figure 6) of the microfluidic flow chamber was able to select the best particle shape for optimal adhesion.

However, microfluidic devices discussed thus far are still idealized constructs that faithfully reproduce the overall size of the microvasculature but do not account for either the true interconnectedness or variations found in the in-vivo microvascular networks. To address this limitation, we have recently developed a novel methodology for accurately reproducing microvascular networks digitized from in vivo images of rodent vasculature onto a microfluidic chip (Figure 7). This “Synthetic Microvascular Network” (SMN) is reproduced from a Geographic Information System (GIS) based mapping of microvascular networks obtained by intra-vital microscopy (Nyguen et al., 2000; Roth et al., 1999). We have shown that this microvascular network based microfluidic device can be cultured with cells and used to study adhesion profiles of functionalized particles (Prabhakarbandian et al., 2011; Rosano et al., 2009; Prabhakarbandian, et al., 2008) in conditions mimicking physiological flow. For example, adhesion of anti-ICAM-1 coated particles on TNF- α activated endothelial cells was found to be 79% and 161% more compared to control IgG coated particles at 4 hour and 24 hour post activation, respectively. We also demonstrated that SMN can predict the adhesion patterns of cells in vivo (Tousi et al., 2010) and showed that bifurcations are the focal points of particle adhesion in microvascular networks (Prabhakarbandian et al., 2011). Cells and microspheres preferentially adhered at significantly higher numbers (>1.5X) near bifurcations and were localized within 1–2 diameters of the bifurcation. This fundamental understanding of the complex cellparticle adhesion would not have been possible without these microvascular network based microfluidic devices.

Flow conditions in interconnected microvascular networks in vivo cannot be accurately described by simple mathematical formulas. Therefore, more sophisticated analytical tools are required for analysis of results from microfluidic devices as they become more realistic, approaching that of the in vivo networks as in the case of SMN described above. Computational Fluid Dynamics (CFD) based modeling provides a powerful tool for describing and predicting fluid flow patterns in microvascular networks. Although numerical analysis of flows dates to the 1800’s, it was only in the early 1980s that CFD modeling became prominent for design and analysis of complex fluid flow and transport systems. These models were subsequently expanded to heat transfer, particle motion and, more recently, to studies of biochemical interactions with multi-physics modules (Prabhakarbandian et al., 2011, 2008; Wang et al., 2009). CFD models have also provided guidance on flow fields for various microfluidic device studies ranging from simple bifurcating structures to complex geometrical structures. For example, CFD modeling of the effects of diverse constructs on cell adhesion has shown that curved channels result in more uniform cell adhesion at bifurcations compared to sharp turn channels (Green et al., 2009). In addition, we have shown that the experimentally observed perfusion profiles (Figure 8)

and adhesion of functionalized particles in SMN in vitro can be successfully predicted by CFD simulations (Prabhakarbandian et al., 2011, 2008). The adhesion patterns obtained from SMN in combination with the fluidic shear predictions from CFD models can be subsequently used to generate shear adhesion maps (Prabhakarbandian et al., 2008).

All of the microfluidic devices discussed so far in this review are two dimensional in nature in that all vessels are located on the same plane and only a single cell type can be cultured in these channels. To address these limitations, Lim et al., 2006 used direct write laser technology to create channels that varied in depth at regular intervals (Figure 9). However, even this device did not accurately reproduce the in vivo 3D environment where vessels often cross each other at different planes and the vascular system contains multiple cell types including endothelial cells, fibroblasts, and smooth-muscle cells. Despite all the limitations of these microfluidic devices, they have achieved significant reductions in the reagent consumption while more accurately modeling the in vivo conditions. Table 1 shows summary of how different configurations of the fluidic chambers compare for the reagent consumptions for a typical adhesion experiment.

6. 3D Microfluidic Devices

Recently, 3D microfluidic devices have been created using PDMS constructs (Zhang et al., 2010) by stacking of individual layers. In addition, 3D scaffolds created using microfabrication techniques and growth matrix gels such as collagen and matrigel (Peltola et al., 2008; Andersson & van den Berg, 2004) have been used to culture multi-layers of cells in these devices (Shin et al., 2004). However, these devices work well only for simplified network geometries because of the difficulties in aligning the different layers of the cells. Recently Hoganson et al., 2010 utilized micromachining procedures and PDMS (Figure 10) to create an idealized in vitro model of lung microvascular system. Even though this device was not based on a realistic microvascular network, it did provide an in vitro model for studying the effects of large changes in shear rates, vessel diameter relationships between parent and daughter vessels, branching angles, vessel length and aspect ratio of vessels. This device also utilized a thin gas exchange membrane made up of silicone and an adjacent alveolar chamber for oxygen flow mimicking in vivo conditions. This type of geometry, where a tissue compartment is adjacent to a vascular compartment, closely resembles conditions in many organs of the body. This approach can be used to, for example, model tumor parenchyma and the vasculature that supplies it, cardiac myocytes nourished by the capillaries, and the tight junctions of the blood-brain barrier. Hence, true 3D in vitro models of microvasculature need to account not only for the interconnectedness of the vascular supply but also for the co-culture of tissue and vascular cells for realistic interaction studies.

7. Imaging Tools

Real time imaging is a critical requirement for understanding the physiological cell-cell and cell-particle interactions. While routinely used imaging methods such as phase contrast microscopy and fluorescence microscopy are better suited for 2D models, methods such as confocal microscopy, multiphoton microscopy and optical coherence tomography enable imaging of 3D models (Graf and Boppart 2010). A detailed review of current methods of imaging microfluidic devices and their advantages and disadvantages are beyond the scope of this paper. However, these techniques with emphasis on 3D imaging have been summarized elsewhere (Smith et al., 2010). Recently, Hearnden et al., 2011 showed that diffusion of nanoparticle can be tracked in a 3D tissue construct using confocal laser scanning microscopy and Rey et al., 2009 used optical coherence tomography to track real-time cell migration. However, both these studies were conducted on static cell culture

models and their application for tracking cells and particles in fluidic 3D environments is not clear.

CONCLUSIONS

Meso-scale parallel plate flow chambers have been used for more than 2 decades for particle adhesion studies. These devices have been instrumental in our efforts to better understand the role of shear forces in the microvasculature but have significant limitations due to the fact that they have nonrealistic morphologies and often require large volumes of reagents. During the past decade microfabrication techniques have been used to develop a number of microfluidic devices to address these limitations. Recently more realistic microfluidic devices that better mimic the in vivo conditions have been developed. However, these devices are still two dimensional in nature and lack many of the geometrical and cellular features of microvascular networks. Development of simplified 3D devices represent a significant advancement in our efforts to produce in vitro models of microvasculature and the tissue that surrounds it. Recent advancements in microfabrication technology and incorporation of various tissue engineering principles herald the emergence of a true 3D mimic of the microvascular system in the near future.

Creation of true 3D microvascular networks based on in vivo images would require novel developments in microfabrication and tissue engineering such as the use of stereolithography and degradable polymers for creation of 3D microfluidic devices. However, a critical component still lacking is the ability for real-time imaging of 3D microvascular networks and their surrounding tissues. Current microvascular imaging technologies only allow stacking of successive 2D images to create a 3D stack, but this process usually limits our understanding of particle-particle and cell-particle interactions. The simultaneous development of 3D microvascular imaging techniques along with capabilities for real-time observation of cell-cell and particle-cell interactions will lead the way for the development of microfluidic devices that can truly mimic in vivo conditions for investigative studies.

Acknowledgments

This work was supported by grants from the National Institutes of Health, the American Heart Association, and the Pennsylvania Department of Health.

REFERENCES

1. Abdelgawad M, Wu C, Chien WY, Geddie WR, Jewett MA, Sun Y. A fast and simple method to fabricate circular microchannels in polydimethylsiloxane (PDMS). *Lab Chip*. 2011; 11(3):545–551.
2. Agrawal N, Toner M, Irimia D. Neutrophil migration assay from a drop of blood. *Lab Chip*. 2008; 8(12):2054–2061. [PubMed: 19023468]
3. Aigner S, Ramos CL, Hafezi-Moghadam A, Lawrence MB, Friederichs J, Altevogt P, Ley K. CD24 mediates rolling of breast carcinoma cells on P-selectin. *FASEB J*. 1998; 12(12):1241–1251. [PubMed: 9737727]
4. Alves CS, Burdick MM, Thomas SN, Pawar P, Konstantopoulos K. The dual role of CD44 as a functional P-selectin ligand and fibrin receptor in colon carcinoma cell adhesion. *Am J Physiol Cell Physiol*. 2008; 294(4):C907–C916. [PubMed: 18234849]
5. Anderson JR, Chiu DT, Jackman RJ, Cherniavskaya O, McDonald JC, Wu H, Whitesides SH, Whitesides GM. Fabrication of topologically complex three-dimensional microfluidic systems in PDMS by rapid prototyping. *Anal Chem*. 2000; 72(14):3158–3164.
6. Andersson H, van den Berg A. Microfabrication and microfluidics for tissue engineering: state of the art and future opportunities. *Lab Chip*. 2004; 4:98–103. [PubMed: 15052347]

7. Barber RW, Emerson DR. Biomimetic design of artificial micro-vasculatures for tissue engineering. *Altern Lab Anim.* 2010; 38 Suppl 1:67–79. Review. [PubMed: 21275485]
8. Bevilacqua MP. Endothelial-leukocyte adhesion molecules. *Annu Rev Immunol.* 1993; 11:767–804. [PubMed: 8476577]
9. Bhatia SK, King MR, Hammer DA. The state diagram for cell adhesion mediated by two receptors. *Biophys J.* 2003; 84(4):2671–2690. [PubMed: 12668476]
10. Blackwell JE, Dagia NM, Dickerson JB, Berg EL, Goetz DJ. Ligand coated nanosphere adhesion to E- and P-selectin under static and flow conditions. *Ann Biomed Eng.* 2001; 29(6):523–533. [PubMed: 11459346]
11. Borenstein JT, Tupper MM, Mack PJ, Weinberg EJ, Khalil AS, Hsiao J, García-Cardena G. Functional endothelialized microvascular networks with circular cross-sections in a tissue culture substrate. *Biomed Microdevices.* 2010; 12(1):71–79. [PubMed: 19787455]
12. Brevig T, Krühne U, Kahn RA, Ahl T, Beyer M, Pedersen LH. Hydrodynamic guiding for addressing subsets of immobilized cells and molecules in microfluidic systems. *BMC Biotechnol.* 2003; 3:10. [PubMed: 12875662]
13. Brown DC, Larson RS. Improvements to parallel plate flow chambers to reduce reagent and cellular requirements. *BMC Immunology.* 2001; 2:9. [PubMed: 11580861]
14. Burdick MM, McCarty OJ, Jadhav S, Konstantopoulos K. Cell-cell interactions in inflammation and cancer metastasis. *IEEE Eng Med Biol Mag.* 2001; 20(3):86–91. [PubMed: 11446216]
15. Butler LM, McGettrick HM, Nash GB. Static and dynamic assays of cell adhesion relevant to the vasculature. *Methods Mol Biol.* 2009; 467:211–228. [PubMed: 19301673]
16. Cao J, Donell B, Deaver DR, Lawrence MB, Dong C. In vitro side-view imaging technique and analysis of human T-leukemic cell adhesion to ICAM-1 in shear flow. *Microvasc Res.* 1998; 55(2):124–137. [PubMed: 9521887]
17. Carlos TM, Harlan JM. Leukocyte-endothelial adhesion molecules. *Blood.* 1994; 84:2068–2101. [PubMed: 7522621]
18. Champion JA, Katare YK, Mitragotri S. Making polymeric micro- and nanoparticles of complex shapes. *Proc Natl Acad Sci U S A.* 2007; 104(29):11901–11904. [PubMed: 17620615]
19. Champion JA, Mitragotri S. Shape induced inhibition of phagocytosis of polymer particles. *Pharm Res.* 2009; 26(1):244–249. [PubMed: 18548338]
20. Chang KC, Tees DF, Hammer DA. The state diagram for cell adhesion under flow: leukocyte rolling and firm adhesion. *Proc Natl Acad Sci U S A.* 2000; 97(21):11262–11267. [PubMed: 11005837]
21. Chapman G, Cokelet G. Model studies of leukocyte-endothelium-blood interactions. I. The fluid flow drag force on the adherent leukocyte. *Biorheology.* 1996; 33(2):119–138. [PubMed: 8679960]
22. Chapman GB, Cokelet GR. Model studies of leukocyte-endothelium-blood interactions. II. Hemodynamic impact of leukocytes adherent to the wall of post-capillary vessels. *Biorheology.* 1997; 34(1):37–56. [PubMed: 9176589]
23. Chiu JJ, Wang DL, Chien S, Skalak R, Usami S. Effects of disturbed flow on endothelial cells. *J Biomech Eng.* 1998; 120(1):2–8. [PubMed: 9675673]
24. Cokelet GR, Soave R, Pugh G, Rathbun L. Fabrication of in vitro microvascular blood flow systems by photolithography. *Microvasc Res.* 1993; 46(3):394–400. [PubMed: 8121322]
25. Conant CG, Schwartz MA, Ionescu-Zanetti C. Well plate-coupled microfluidic devices designed for facile image-based cell adhesion and transmigration assays. *J Biomol Screen.* 2010; 15(1):102–106. [PubMed: 19965806]
26. Cozens-Roberts C, Quinn JA, Lauffenberger DA. Receptor-mediated adhesion phenomena. Model studies with the Radical-Flow Detachment Assay *Biophys J.* 1990; 58(1):107–125.
27. Crutchfield KL, Shinde Patil VR, Campbell CJ, Parkos CA, Allport JR, Goetz DJ. CD11b/CD18-coated microspheres attach to E-selectin under flow. *J Leukoc Biol.* 2000; 67(2):196–205. [PubMed: 10670580]
28. Diamond MS, Springer TA. The dynamic regulation of integrin adhesiveness. *Curr Biol.* 1. 1994; 4(6):506–517. Review.

29. Dickerson JB, Blackwell JE, Ou JJ, Shinde Patil VR, Goetz DJ. Limited adhesion of biodegradable microspheres to E- and P-selectin under flow. *Biotechnol Bioeng.* 2001; 73(6):500–509. [PubMed: 11344455]
30. Doshi N, Mitragotri S. Macrophages recognize size and shape of their targets. *PLoS One.* 2010; 5(4) e10051.
31. Doshi N, Prabhakarandian B, Rea-Ramsey A, Pant K, Sundaram S, Mitragotri S. Flow and adhesion of drug carriers in blood vessels depend on their shape: a study using model synthetic microvascular networks. *J Control Release.* 2010; 146(2):196–200. [PubMed: 20385181]
32. Ebnet K, Vestweber D. Molecular mechanisms that control leukocyte extravasation: the selectins and the chemokines. *Histochem Cell Biol.* 1999; 112(1):1–23. Review. [PubMed: 10461808]
33. Farokhzad OC, Khademhosseini A, Jon S, Herrmann A, Cheng J, Chin C, Kiselyuk A, Teply B, Eng G, Langer R. Microfluidic system for studying the interaction of nanoparticles and microparticles with cells. *Anal Chem.* 2005; 77(17):5453–5459. [PubMed: 16131052]
34. Fiddes LK, Raz N, Srigunapalan S, Tumarkan E, Simmons CA, Wheeler AR, Kumacheva E. A circular cross-section PDMS microfluidics system for replication of cardiovascular flow conditions. *Biomaterials.* 2010; 13:3459–3464. [PubMed: 20167361]
35. Fillafer C, Ratzinger G, Neumann J, Guttenberg Z, Dissauer S, Lichtscheidl IK, Wirth M, Gabor F, Schneider MF. An acoustically-driven biochip - impact of flow on the cell-association of targeted drug carriers. *Lab Chip.* 2009; 9(19):2782–2788. [PubMed: 19967114]
36. Frame MD, Sarelius IH. A system for culture of endothelial cells in 20–50-microns branching tubes. *Microcirculation.* 1995; 2(4):377–385. [PubMed: 8714819]
37. Goetz DJ, el-Sabban ME, Pauli BU, Hammer DA. Dynamics of neutrophil rolling over stimulated endothelium in vitro. *Biophys J.* 1994; 66(6):2202–2209. [PubMed: 7521229]
38. Graf BW, Boppart SA. Imaging and analysis of three-dimensional cell culture models. *Methods Mol Biol.* 2010; 591:211–227. [PubMed: 19957133]
39. Granger DN, Rodrigues SF, Yildirim A, Senchenkova EY. Microvascular responses to cardiovascular risk factors. *Microcirculation.* 2010; 17(3):192–205. Review. [PubMed: 20374483]
40. Green JV, Kniazeva T, Abedi M, Sokhey DS, Taslim ME, Murthy SK. Effect of channel geometry on cell adhesion in microfluidic devices. *Lab Chip.* 2009; 9(5):677–685. [PubMed: 19224017]
41. Hammer DA, Apte SM. Simulation of cell rolling and adhesion on surfaces in shear flow: general results and analysis of selectin-mediated neutrophil adhesion. *Biophys J.* 1992; 63(1):35–57. [PubMed: 1384734]
42. Hammer DA, Lauffenburger DA. A dynamical model for receptor-mediated cell adhesion to surfaces in viscous shear flow. *Cell Biophys.* 1989; 14(2):139–173. [PubMed: 2472206]
43. Hammer DA, Lauffenburger DA. A dynamical model for receptor-mediated cell adhesion to surfaces. *Biophys J.* 1987; 52(3):475–487. [PubMed: 2820521]
44. Hearnden V, MacNeil S, Battaglia G. Tracking nanoparticles in three-dimensional tissue-engineered models using confocal laser scanning microscopy. *Methods Mol Biol.* 2011; 695:41–51. [PubMed: 21042964]
45. Hoganson DM, Pryor HI 2nd, Bassett EK, Spool ID, Vacanti JP. Lung assist device technology with physiologic blood flow developed on a tissue engineered scaffold platform. *Lab Chip.* 2011; 11(4):700–707. [PubMed: 21152606]
46. Humphries MJ. Cell adhesion assays. *Methods Mol Biol.* 2009; 522:203–210. [PubMed: 19247616]
47. Jackson SP, Nesbitt WS, Westein E. Dynamics of platelet thrombus formation. *J Thromb Haemost.* 2009 Suppl 1:17–20. Review. [PubMed: 19630759]
48. Jain A, Munn LL. Determinants of leukocyte margination in rectangular microchannels. *PLoS One.* 2009; 4(9) e7104.
49. Kang S, Park T, Chen X, Dickens G, Lee B, Lu K, Rakhilin N, Daniel S, Jin MM. Tunable physiologic interactions of adhesion molecules for inflamed cell-selective drug delivery. *Biomaterials.* 2011; 32(13):3487–3498. [PubMed: 21306773]
50. Karunarathne W, Ku CJ, Spence DM. The dual nature of extracellular ATP as a concentration-dependent platelet P2X1 agonist and antagonist. *Integr Biol (Camb).* 2009; 11(12):655–663. [PubMed: 20027374]

51. Kendall RA, Alhnan MA, Nilkumhang S, Murdan S, Basit AW. Fabrication and in vivo evaluation of highly pH-responsive acrylic microparticles for targeted gastrointestinal delivery. *Eur J Pharm Sci.* 2009; 37(3–4):284–290. [PubMed: 19491017]
52. Kiani MF, Yuan H, Chen X, Smith L, Gaber MW, Goetz DJ. Targeting microparticles to select tissue via radiation-induced upregulation of endothelial cell adhesion molecules. *Pharm Res.* 2002; 19(9):1317–1322. [PubMed: 12403068]
53. Kotz KT, Xiao W, Miller-Graziano C, Qian WJ, Russom A, Warner EA, Moldawer LL, De A, Bankey PE, Petritis BO, Camp DG 2nd, Rosenbach AE, Goverman J, Fagan SP, Brownstein BH, Irimia D, Xu W, Wilhelmy J, Mindrinos MN, Smith RD, Davis RW, Tompkins RG, Toner M. Clinical microfluidics for neutrophil genomics and proteomics. Inflammation and the Host Response to Injury Collaborative Research Program. *Nat Med.* 2010; 16(9):1042–1047. [PubMed: 20802500]
54. Kumari A, Yadav SK, Yadav SC. Biodegradable polymeric nanoparticles based drug delivery systems. *Colloids Surf B Biointerfaces.* 2010; 75(1):1–18. Review. [PubMed: 19782542]
55. Lawrence MB, McIntire LV, Eskin SG. Effect of flow on polymorphonuclear leukocyte/ endothelial cell adhesion. *Blood.* 1987; 70:1284–1290. [PubMed: 3663936]
56. Leyton-Mange J, Yang S, Hoskins MH, Kunz RF, Zahn JD, Dong C. Design of a side-view particle imaging velocimetry flow system for cell-substrate adhesion studies. *J Biomech Eng.* 2006; 128(2):271–278. [PubMed: 16524340]
57. Lim D, Kamotani Y, Cho B, Mazumder J, Takayama S. Fabrication of microfluidic mixers and artificial vasculatures using a high-brightness diode-pumped Nd:YAG laser direct write method. *Lab Chip.* 2003; 3(4):318–323. [PubMed: 15007466]
58. Luscinskas FW, Kansas GS, Ding H, Pizcueta P, Schleiffenbaum B, Tedder TF, Gimbrone MA Jr. Monocyte rolling, arrest and spreading on IL-4-activated vascular endothelium under flow is mediated via sequential action of L-selectin, beta-1 -integrins, and beta-2-integrins. *J. Cell Biol.* 1994; 125:1417–1427. [PubMed: 7515891]
59. Luscinskas FW, Gimbrone MA Jr. Endothelial-dependent mechanisms in chronic inflammatory leukocyte recruitment. *Annu Rev Med.* 1996; 47:413–421. Review. [PubMed: 8712792]
60. Mateu MG. Virus engineering: functionalization and stabilization. *Protein Eng Des Sel.* 2011; 24(1–2):53–63. [PubMed: 20923881]
61. Muro S, Garnacho C, Champion JA, Leferovich J, Gajewski C, Schuchman EH, Mitragotri S, Muzykantov VR. Control of endothelial targeting and intracellular delivery of therapeutic enzymes by modulating the size and shape of ICAM-1-targeted carriers. *Mol Ther.* 2008; 16(8):1450–1458. [PubMed: 18560419]
62. Murthy SK, Sin A, Tompkins RG, Toner M. Effect of flow and surface conditions on human lymphocyte isolation using microfluidic chambers. *Langmuir.* 2004; 20(26):11649–11655. [PubMed: 15595794]
63. Muzykantov VR. Drug delivery by red blood cells: vascular carriers designed by mother nature. *Expert Opin Drug Deliv.* 2010; 7(4):403–427. Review. [PubMed: 20192900]
64. Nalayanda DD, Kalukanimuttam M, Schmidtke DW. Micropatterned surfaces for controlling cell adhesion and rolling under flow. *Biomed Microdevices.* 2007; 9(2):207–214. [PubMed: 17160704]
65. Neeves KB, Maloney SF, Fong KP, Schmaier AA, Kahn ML, Brass LF, Diamond SL. Microfluidic focal thrombosis model for measuring murine platelet deposition and stability: PAR4 signaling enhances shear-resistance of platelet aggregates. *J Thromb Haemost.* 2008; 6(12):2193–2201. [PubMed: 18983510]
66. Nguyen V, Gaber MW, Sontag MR, Kiani MF. Late effects of ionizing radiation on the microvascular networks in normal tissue. *Radiat Res.* 2000; 154(5):531–56. [PubMed: 11025649]
67. Paprocka M, Duš D, Mitterrand M, Lamerant-Fayel N, Kieda C. Flow cytometric assay for quantitative and qualitative evaluation of adhesive interactions of tumor cells with endothelial cells. *Microvasc Res.* 2008; 76(2):134–138. [PubMed: 18675997]
68. Patel KD. Mechanisms of selective leukocyte recruitment from whole blood on cytokine-activated endothelial cells under flow conditions. *J Immunol.* 1999; 162(10):6209–6216. [PubMed: 10229866]

69. Pattillo CB, Venegas B, Donelson FJ, Del Valle L, Knight LC, Chong PL, Kiani MF. Radiation-guided targeting of combretastatin encapsulated immunoliposomes to mammary tumors. *Pharm.Res.* 2009; 26(5):1093–1100. [PubMed: 19172383]
70. Peltola SM, Melchels FPW, Grijpma DW, Kellomäki M. A review of rapid prototyping techniques for tissue engineering purposes. *Annals of Medicine.* 2008; 40(4):268–280. [PubMed: 18428020]
71. Peramo A, Meads MB, Dalton WS, Matthews WG. Static adhesion of cancer cells to glass surfaces coated with glycosaminoglycans. *Colloids Surf B Biointerfaces.* 2008; 67(1):140–144. [PubMed: 18815015]
72. Petrelli F, Borgonovo K, Barni S. Targeted delivery for breast cancer therapy: the history of nanoparticle-albumin-bound paclitaxel. *Expert Opin Pharmacother.* 2010; 11(8):1413–1432. [PubMed: 20446855]
73. Prabhakarbandian B, Pant K, Scott RC, Patillo CB, Irimia D, Kiani MF, Sundaram S. Synthetic microvascular networks for quantitative analysis of particle adhesion. *Biomed Microdevices.* 2008; 10(4):585–595. [PubMed: 18327641]
74. Prabhakarbandian B, Wang Y, Rea-Ramsey A, Sundaram S, Kiani MF, Pant K. Bifurcations: Focal Points of Particle Adhesion in Microvascular Networks. *Microcirculation.* 2011 Mar 19. [Epub ahead of print].
75. Prabhakarbandian B, Swerlick RA, Goetz DJ, Kiani MF. Expression and Functional Significance of E-selectin on Cultured Endothelial Cells in Response to Ionizing Radiation. *Microcirculation.* 2001; 8:355–364. [PubMed: 11687947]
76. Rey SM, Povazay B, Hofer B, Unterhuber A, Hermann B, Harwood A, Drexler W. Three- and four-dimensional visualization of cell migration using optical coherence tomography. *J Biophotonics.* 2009; 2(6–7):370–379. [PubMed: 19475627]
77. Rosano JM, Touse N, Scott RC, Krynska B, Rizzo V, Prabhakarbandian B, Pant K, Sundaram S, Kiani MF. A physiologically realistic in vitro model of microvascular networks. *Biomed Microdevices.* 2009; 11(5):1051–1057.
78. Roth NM, Kiani MF. A "geographic information systems" based technique for the study of microvascular networks. *Ann Biomed Eng.* 1999; 27(1):42–47. [PubMed: 9916759]
79. Rouleau L, Copland IB, Tardif JC, Mongrain R, Leask RL. Neutrophil adhesion on endothelial cells in a novel asymmetric stenosis model: effect of wall shear stress gradients. *Ann Biomed Eng.* 2010; 38(9):2791–2804. [PubMed: 20387119]
80. Ruel J, Lemay J, Dumas G, Doillon C, Charara J. Development of a parallel plate flow chamber for studying cell behavior under pulsatile flow. *ASAIO J.* 1995; 41(4):876–883. [PubMed: 8589470]
81. Runyon MK, Johnson-Kerner BL, Ismagilov RF. Minimal functional model of hemostasis in a biomimetic microfluidic system. *Angew Chem Int Ed Engl.* 2004; 43(12):1531–1536. [PubMed: 15022225]
82. Sakhalkar HS, Dalal MK, Salem AK, Ansari R, Fu J, Kiani MF, Kurjiaka DT, Hanes J, Shakesheff KM, Goetz DJ. Leukocyte-inspired biodegradable particles that selectively and avidly adhere to inflamed endothelium in vitro and in vivo. *Proc Natl Acad Sci U S A.* 2003; 100(26):15895–15900. [PubMed: 14668435]
83. Schaff UY, Xing MM, Lin KK, Pan N, Jeon NL, Simon SI. Vascular mimetics based on microfluidics for imaging the leukocyte--endothelial inflammatory response. *Lab Chip.* 2007; 7(4):448–456. [PubMed: 17389960]
84. Scott RC, Rosano JM, Ivanov Z, Wang B, Chong PLG, Issekutz AC, Crabbe D, Kiani MF. Targeting VEGF-encapsulated immunoliposomes to MI heart improves vascularity and cardiac function. *FASEB J.* 2009; 23:3361–3367. [PubMed: 19535683]
85. Shen F, Kastrop CJ, Liu Y, Ismagilov RF. Threshold response of initiation of blood coagulation by tissue factor in patterned microfluidic capillaries is controlled by shear rate. *Arterioscler Thromb Vasc Biol.* 2008; 28(11):2035–2041. [PubMed: 18703776]
86. Shin M, Matsuda K, Ishii O, Terai H, Kaazempur-Mofrad M, Borenstein J, Detmar M, Vacanti JP. Endothelialized networks with a vascular geometry in microfabricated poly(dimethyl siloxane). *Biomed Microdevices.* 2004; 6(4):269–278. [PubMed: 15548874]

87. Sia SK, Whitesides GM. Microfluidic devices fabricated in poly(dimethylsiloxane) for biological studies. *Electrophoresis*. 2003; 24(21):3563–3576. Review. [PubMed: 14613181]
88. Simon SI, Goldsmith HL. Leukocyte adhesion dynamics in shear flow. *Ann Biomed Eng*. 2002; 30(3):315–332. Review. [PubMed: 12051617]
89. Smith LE, Smallwood R, Macneil S. A comparison of imaging methodologies for 3D tissue engineering. *Microsc Res Tech*. 2010; 73(12):1123–1133. [PubMed: 20981758]
90. Sperandio M, Pickard J, Unnikrishnan S, Acton ST, Ley K. Analysis of leukocyte rolling in vivo and in vitro. *Methods Enzymol*. 2006; 416:346–371. [PubMed: 17113878]
91. Springer TA. Traffic signals for lymphocyte recirculation leukocyte emigration: the multistep paradigm. *Cell*. 1994; 76:301–314. [PubMed: 7507411]
92. Totani L, Evangelista V. Platelet-leukocyte interactions in cardiovascular disease and beyond. *Arterioscler Thromb Vasc Biol*. 2010; 30(12):2357–2361. Review. [PubMed: 21071701]
93. Tousi N, Wang B, Pant K, Kiani MF, Prabhakarbandian B. Preferential adhesion of leukocytes near bifurcations is endothelium independent. *Microvasc Res*. 2010; 80(3):384–388. [PubMed: 20624406]
94. Tovar-Lopez FJ, Rosengarten G, Westein E, Khoshmanesh K, Jackson SP, Mitchell A, Nesbitt WS. A microfluidics device to monitor platelet aggregation dynamics in response to strain rate micro-gradients in flowing blood. *Lab Chip*. 2010; 10(3):291–302. [PubMed: 20091000]
95. Tözere A, Kleinman HK, Grant DS, Morales D, Mercurio AM, Byers SW. E-selectin-mediated dynamic interactions of breast- and colon-cancer cells with endothelial-cell monolayers. *Int J Cancer*. 1995; 60(3):426–431. [PubMed: 7530236]
96. Tran L, Farinas J, Ruslim-Litrus L, Conley PB, Muir C, Munnely K, Sedlock DM, Cherbavaz DB. Agonist-induced calcium response in single human platelets assayed in a microfluidic device. *Anal Biochem*. 2005; 341(2):361–368. [PubMed: 15907883]
97. Usami S, Chen HH, Zhao Y, Chien S, Skalak R. Design and construction of a linear shear stress flow chamber. *Ann Biomed Eng*. 1993; 21(1):77–83. [PubMed: 8434823]
98. van der Meer AD, Poot AA, Duits MH, Feijen J, Vermes I. Microfluidic technology in vascular research. *J Biomed Biotechnol*. 2009; 2009 823148. Review.
99. Wang B, Scott RC, Pattillo CB, Prabhakarbandian B, Sundaram S, Kiani MF. Modeling oxygenation and selective delivery of drug carriers post-myocardial infarction. *Adv Exp Med Biol*. 2008; 614:333–343. [PubMed: 18290344]
100. Xiao Y, Truskey GA. Effect of receptor-ligand affinity on the strength of endothelial cell adhesion. *Biophys J*. 1996; 71(5):2869–2884. [PubMed: 8913624]
101. Yoo JW, Mitragotri S. Polymer particles that switch shape in response to a stimulus. *Proc Natl Acad Sci U S A*. 2010; 107(25):11205–11210. [PubMed: 20547873]
102. Zhai G, Wu J, Yu B, Guo C, Yang X, Lee RJ. A transferrin receptor-targeted liposomal formulation for docetaxel. *J Nanosci Nanotechnol*. 2010; 10(8):5129–5136. [PubMed: 21125861]
103. Zhang M, Wu J, Wang L, Xiao K, Wen W. A simple method for fabricating multi-layer PDMS structures for 3D microfluidic chips. *Lab Chip*. 2010; 10(9):1199–1203. [PubMed: 20390140]
104. Zigler M, Dobroff AS, Bar-Eli M. Cell adhesion: implication in tumor progression. *Minerva Med*. 2010; 101(3):149–162. Review. [PubMed: 20562803]

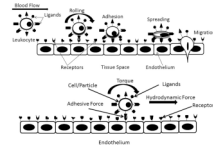


Figure 1.
Particle Adhesion Process

- A.** Schematic of the leukocyte adhesion process. Leukocytes roll on the endothelium followed by adhesion, spreading and subsequent migration into the tissue space
- B.** Example of a common biophysical process during cell Cells/particles adhere when the adhesive forces are equal or greater than the hydrodynamic forces acting on the cell. Although the illustration shows the hydrodynamic force parallel to the surface, the realized force may have a new orientation following rolling the adhesive forces formed between the ligand and receptors will not necessarily be normal to the surface at all times during the adhesion process.

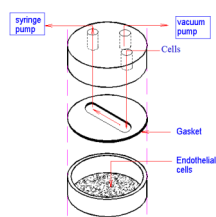


Figure 2.
Schematic of the Glycotech Flow Chamber for studying cellular interaction.

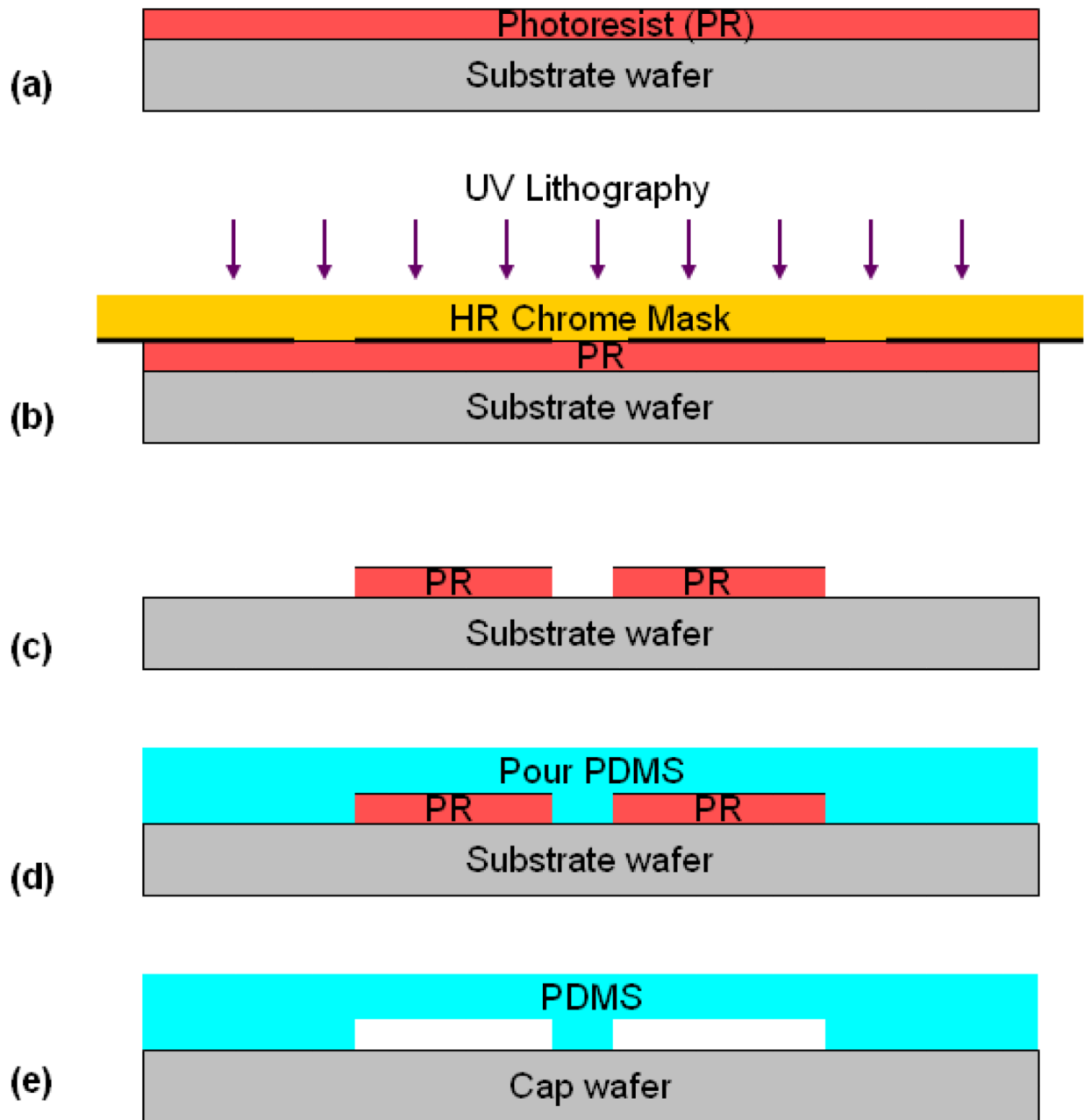


Figure 3.

Fabrication Process of PDMS devices by soft-lithography: (a) Spin-coating of photoresist (PR); (b) UV photolithography of the PR; (c) Development of the PR; (d) PDMS casting over developed PR, followed by PDMS curing; and (e) PDMS bonding to a cap (microscope slides, coverslip, glass, etc.)

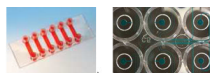


Figure 4.
Idealized Microfluidic Devices currently on the Market

- A. μ -Slide (Ibidi LLC) for adhesion assays
- B. Fluxion Biosciences Well plate based high-throughput assay for adhesion assays

(Reproduced with permission from Ibidi LLC and Fluxion Biosciences)

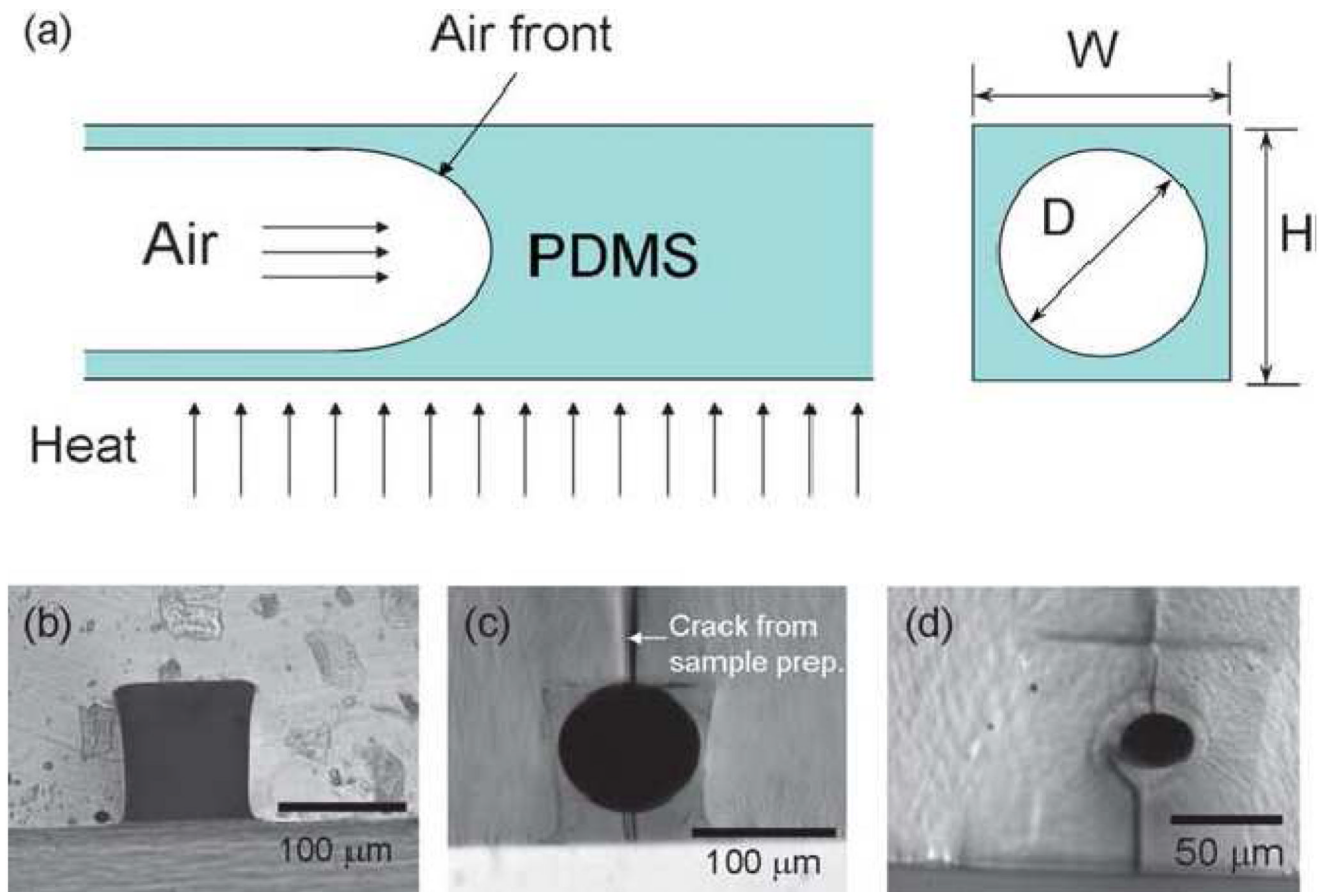


Figure 5.

(a) Schematic of the circular channels fabrication process. (b and c) Picture of a $100\ \mu\text{m} \times 100\ \mu\text{m}$ microchannel before and after treatment. (d) Picture of $100\ \mu\text{m} \times 100\ \mu\text{m}$ channel after coating it three times with liquid PDMS [Abdelgawad et al., 2010]-Reproduced by permission of The Royal Society of Chemistry, <http://dx.doi.org/10.1039/c0lc00093k>

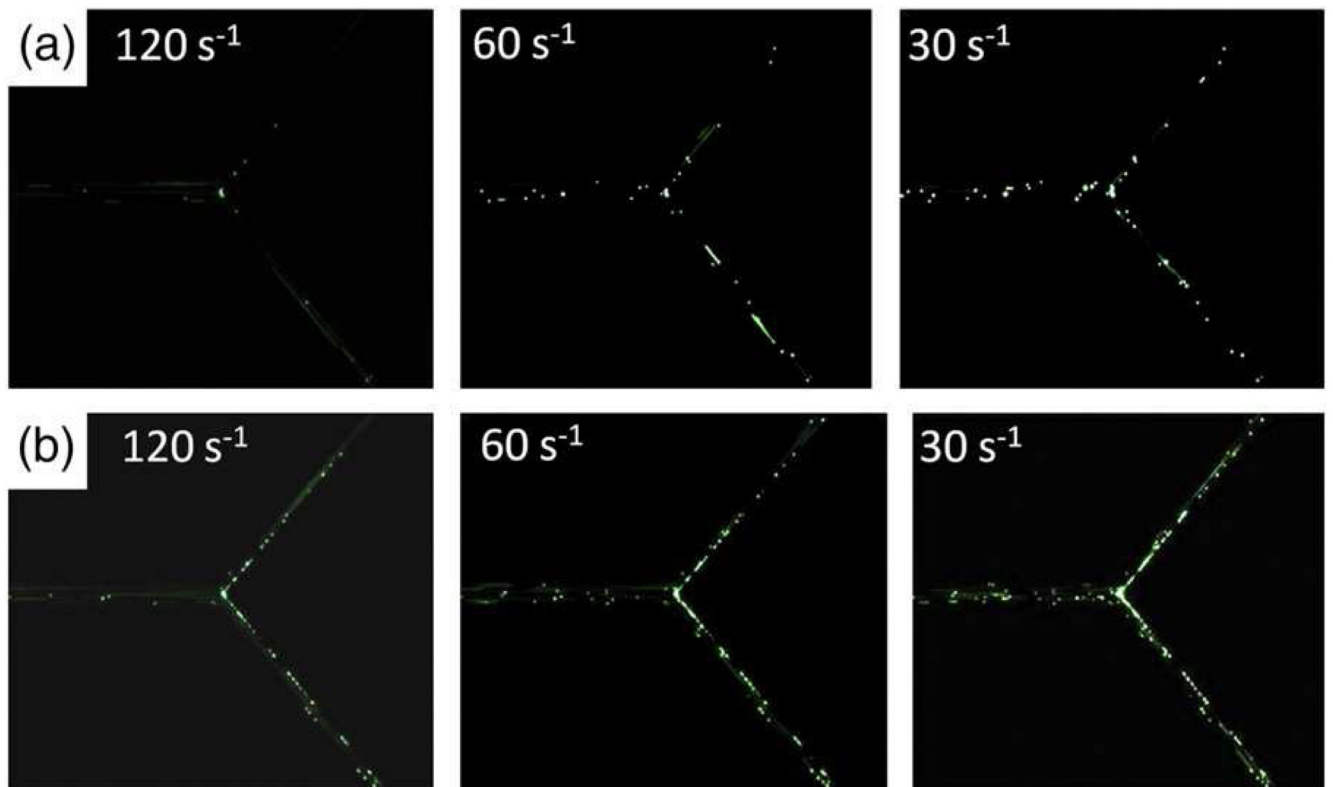


Figure 6. Particle adhesion profiles at the bifurcation and linear sections of a microfluidic device. (a) adhesion patterns of spherical particles (b) adhesion patterns of elliptical particles. Reprinted from *J Control Release*. Sep 1;146 (2), Doshi et al., Flow and adhesion of drug carriers in blood vessels depend on their shape: a study using model synthetic microvascular networks. 196–200 2010 with permission from Elsevier.

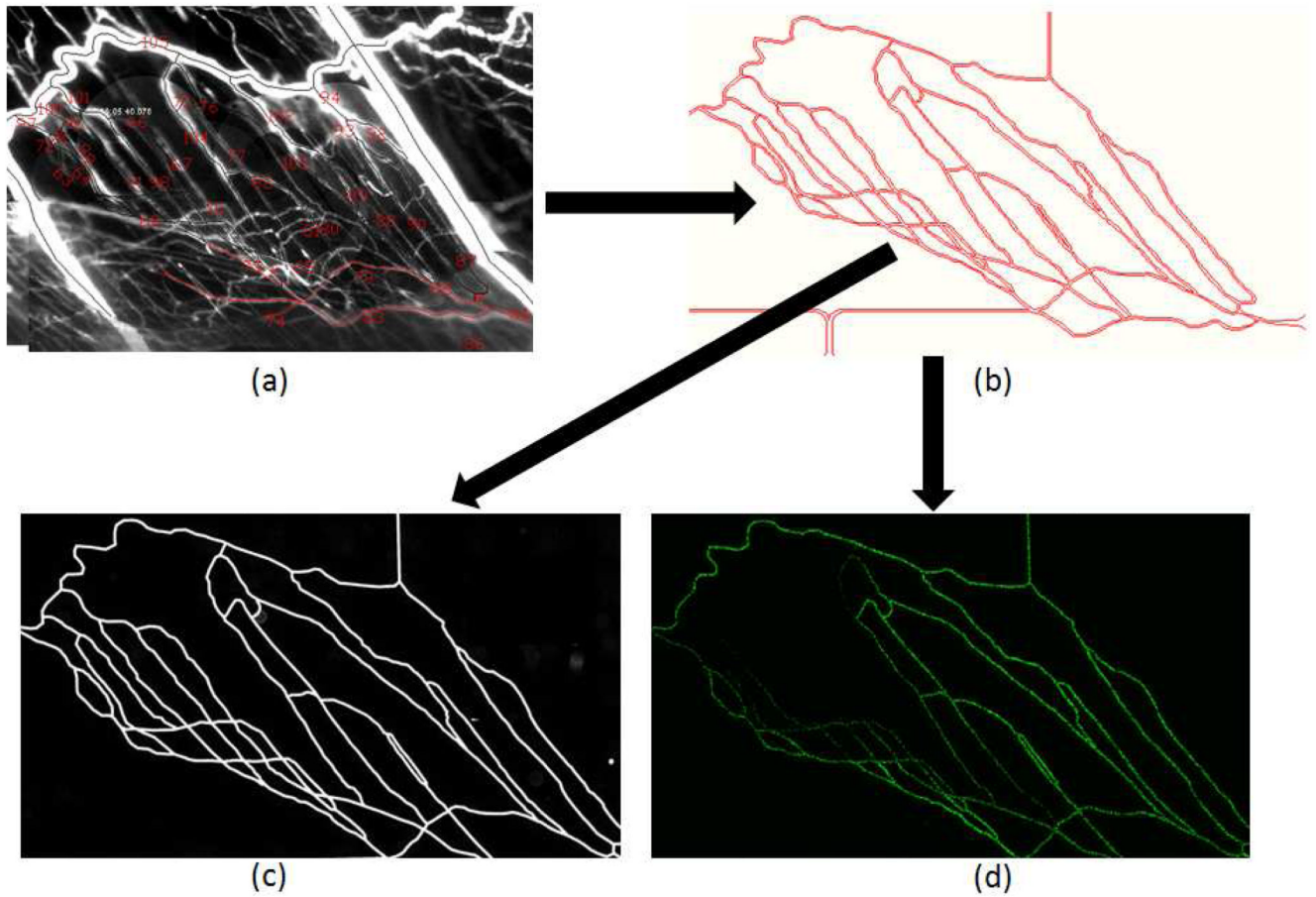


Figure 7. Synthetic Microvascular Network (SMN) based microfluidic chip (a). Image of microvascular network in-vivo perfused with fluorescent rhodamine (b). Digitized AutoCAD image of microvascular network in panel “a” (c). Microfluidic chip perfused with fluorescent dye, (d). Microfluidic chip with perfused fluorescent particles. Intensity of the fluorescent images in panels a, c, and d have been digitally enhanced to better highlight the microvessels/microchannels.

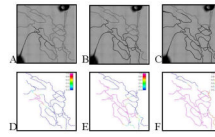


Figure 8.

Transient perfusion studies comparing experimental and simulation results in SMN. (panels A–C) experiments and (panels D–F) CFD simulation. The scale for simulation is an arbitrary unit with blue (no perfusion; 0) and magenta (complete perfusion; 1). Experimental and simulation results show very good comparison with each other. (With kind permission from Springer Science+Business Media:Biomed Microdevices, Synthetic microvascular networks for quantitative analysis of particle adhesion, Aug 10(4), 2008, 585–95, Prabhakarbandian et al., Figure 4)

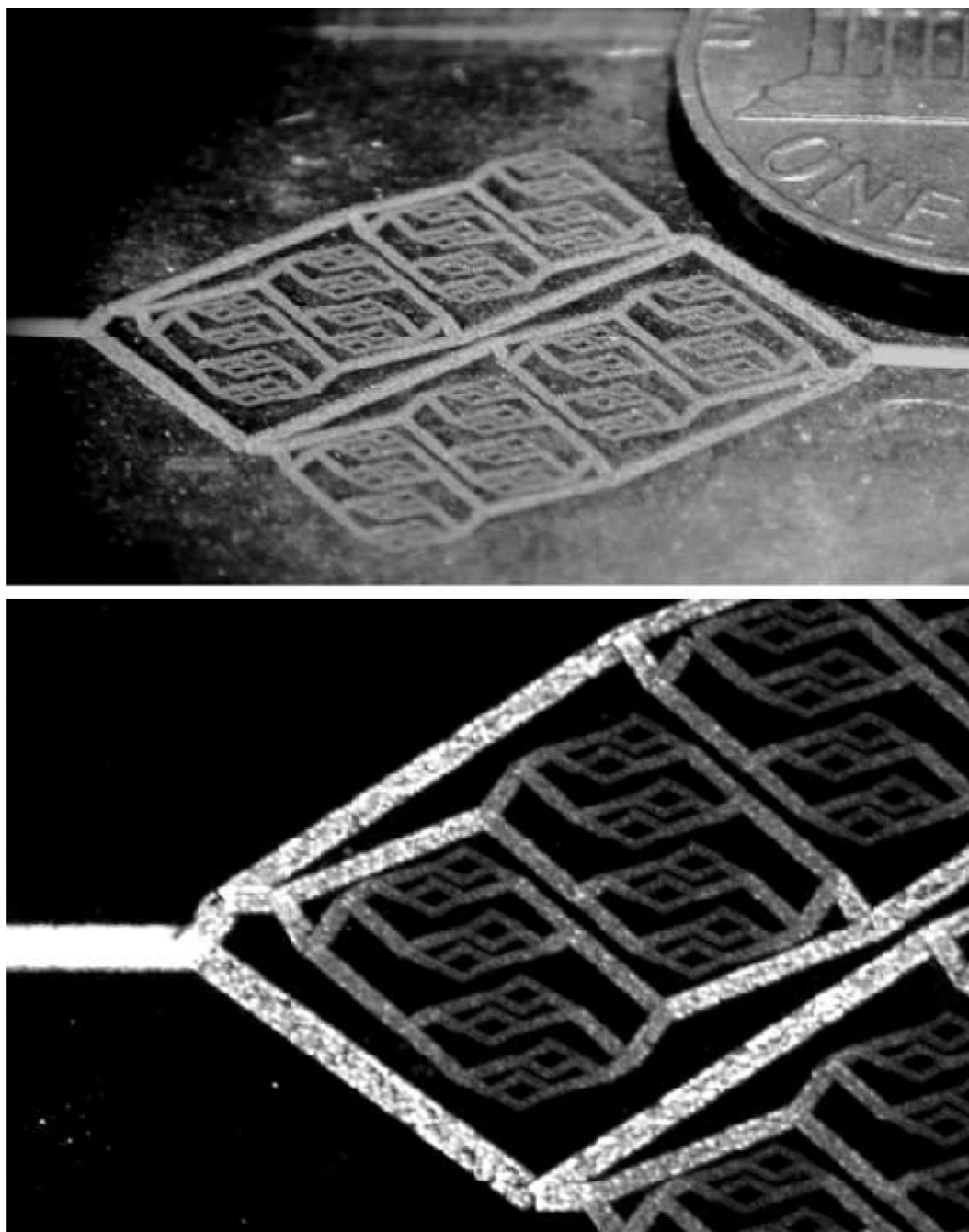


Figure 9. (Top panel) Eight level multi-width multi-level microvasculature network with microchannels fabricated by one-step laser direct write. (Bottom panel) Image showing the difference in intensity levels corresponding to different channel depths [Lim et al., 2003]- Reproduced by permission of The Royal Society of Chemistry, <http://dx.doi.org/10.1039/B308452C>

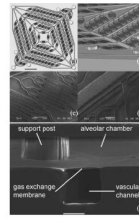


Figure 10.

Design of lung vascular network with physiologic blood flow. (a) Top view of high density vascular network design, (b) isometric view of SolidWorks rendering of mold demonstrating variable depths and 1 : 1 aspect ratios of all channels, (c) SEM of smallest channels of device, (d) SEM of transition between large inlet channel and branch channel demonstrating precise 3D fillets achieved with micro machined mold. Scale bar in (a, c, d) = 1 cm. (e) Isometric cross-sectional view SEM of the device showing the three components of the device; alveolar chamber, gas exchange membrane and vascular network. Scale bar (e) = 100µm [Hoganson et al., 2011]-Reproduced by permission of The Royal Society of Chemistry, <http://dx.doi.org/10.1039/C0LC00158A>

Table 1

Comparison of Reagent Consumption for a Typical Adhesion Experiment

Adhesion Platform	Reagent Volume (μL)	# of Cells/Particles per experiment	Dead Volume (μL)
Parallel Plate Flow Chamber (Glycotech)	50–2000	5E+05	32.0
Microfluidic Flow Chamber (Doshi et al., 2010)	0.05	5E+02	3.0
SMN Flow Chamber (Prabhakarbandian et al., 2008)	1	5E+02	3.0

Note: Values for Glycotech are for a typical assay with a shear rate of 60 sec^{-1} , particle concentration of $1\text{E}6$ particles/ml and duration of 3 min for adhesion. Values for microfluidic and SMN flow chamber are for the same shear rate, particle concentration of $5\text{E}6$ particles/ml, and duration of 10 min for adhesion.